

Finding a Closest Match between Wi-Fi Propagation Measurements and Models

Burjiz Soorty

School of Engineering, Computer and Mathematical
Sciences

Auckland University of Technology

Auckland, New Zealand

burjizsoorty@hotmail.com

Nurul I Sarkar

School of Engineering, Computer and Mathematical
Sciences

Auckland University of Technology

Auckland, New Zealand

nurul.sarkar@aut.ac.nz

Abstract – In a series of papers by Sarkar and his team conducted radio propagation measurements to study the performance of Wi-Fi in terms of received signal strengths (RSS) in an obstructed office block. The goal of this paper is to find a closest match between the results obtained from propagation measurements and the theoretical models. The RSS measurement results are compared with the four selected propagation models (Free-space, Two-ray ground reflection, Shadowing path loss, and the overall Shadowing models). These models were selected based on their popularity and relevance to our study. Results obtained show that the overall shadowing model is the best-fit followed by the path loss Shadowing. We found about 94% and 99% matching with RSS measurement results for non-LOS and NLOS conditions, respectively. The analysis and research findings reported in this paper provide some insights into the deployment of indoor wireless systems.

Keywords: radio propagation measurements, models, free-space, path loss shadowing, overall shadowing model.

I. INTRODUCTION

Sarkar et al. [1-4] have conducted various radio propagation measurements to study the performance of Wi-Fi networks in terms of received signal strength (RSS) values. In this paper we focus on finding a closest match between Sarkar and Lo's [3] propagation measurement results (in an obstructed office block) and the four models (Free-space, Two-Ray Ground Reflection, Shadowing path loss, and the overall Shadowing).

A radio propagation model is an empirical mathematical formulation that characterizes radio wave propagation as a function of frequency, distance and other affecting factors. They are commonly categorized into two segments, namely Large-Scale and Small-Scale radio wave models. Large-Scale models are used to estimate the radio coverage of a transmitter by received signal strength (RSS). The average RSS between the transmitter (TX) and receiver (RX) can thus be determined using Large-Scale propagation models. Small-Scale propagation models are used to estimate the fluctuation of the RSS over short distances ($\sim \lambda$) or short periods of time ($\sim s$).

There are several radio wave models that have been developed depending on the propagation behavior of radio waves in different conditions. These models are broadly categorized as indoor and outdoor propagation models. However, models for outdoor propagation are further subcategorized into Foliage models, Terrain models, and City models where each model is developed depending on a set range of parameters. The indoor propagation models are categorized into free space model, two-ray ground model and shadowing model. The mathematical formulas for these models are discussed in Section IV.

This paper addresses the following research question. What indoor radio propagation model best-fit with the measurement results?

To answer the question posed we compare the RSS measurement results with each of the four indoor models considered. The RSS values for the models were calculated and presented in Section IV

The rest of the paper is organized as follows. Section II reviews relevant literature on indoor radio propagation models. Section III outlines radio propagation environment and measurements. Research findings including propagation models are presented in Section IV. Section V presents analysis of research findings, and a brief conclusion in Section VI concludes the paper.

II. RELATED WORK

This section reviews a set of literature on indoor radio propagation models and measurements.

In 2003, A.H. Muqaibel et al. [5] conducted a study on the propagation of ultra-wideband (UWB) signals in indoor environments. Time-domain indoor propagation measurements using pulses with FWHM (full width at half maximum) equal to 85 ps were carried out. Several indoor conditions were implemented in the WLAN evaluation in order to measure and record results for typically common WLAN scenarios. These included conditions of line-of-sight (LOS), non-line-of-sight (NLOS), room-to-room, within-the-room and hallways. Path-loss exponent and time dispersion were the two parameters for which results of the indoor propagation measurements of local power delay profiles (local PDP) and averaged power delay profiles

(SSA-PDP) were recorded. Their study discussed the statistical analyses of their measured data with earlier published UWB and narrowband results.

In 2004, S. Zvanovec et al. [6] carried out an indoor measurement campaign in the 2.45 GHz ISM frequency band to predict the signal propagation. Two measurement methods were accomplished. The first, narrowband measurement was to find the empirical parameters for COST231 Multi-Wall and One-Slope models to allow mean signal level prediction for initial coverage planning [6]. The second, wideband measurement was focused on the long-term signal power level measurement to investigate statistical distributions of fades. Time variations of WLAN signal level were investigated and the cumulative distribution functions based on log-normal distribution were determined. Their findings revealed that the semi-empirical Multi-Wall model resulted in much better performance than the One-Slope model and was thus favorable for indoor coverage predictions for initial WLAN planning and implementation. In 2005, C.C. Chong et al. [7] measured ultra-wideband (UWB) indoor propagation channels in various types of high-rise apartments located at several cities in Korea in-order to provide insight into UWB propagation-channel modelling purposes. Channel transfer functions in the frequency band of 3-10 GHz were measured using a vector network analyzer and corresponding channel impulse responses were calculated. RX antennas were spread over a range of 1-20 m from the fixed transmitter location in-order to characterize the small-scale and large-scale statistics of the channel. Line-of-sight (LOS) and NLOS conditions were considered and measurements were recorded in the form of power delay and RMS delay spread. Their findings showed that clustering phenomena existed in the temporal domain. Mean and standard deviation of the RMS delay spread increased from LOS to NLOS scenarios as well as with the increase in distance between TX and RX separation.

In 2009, Zeng Dongdong et al. [8] carried out a study on the properties of indoor propagation for mobile communication. Their experiment consisting of a signal generator as a CW transmitter, a spectral analyzer as a receiver and a pair of vertically polarized dipole antennas, were used to measure results in a corridor located at the top floor of a nine storied building. Two scenarios were considered for the layout of the indoor propagation environment where results were measured from two different ‘transmit antennas’ (Tx) placed at two different positions. The ‘Tx’ and ‘Rx’ antennas were placed at a height of 1.1m from the floor for scenario one and 1.0m from the floor for scenario two. Their findings revealed the fluctuation trend to vary depending on the distance from the transmit antenna. In 2010, Yuanyuan Ma and Matthias

Patzold [9] carried out a propagation study on the design and simulation of narrowband indoor propagation channels under LOS and NLOS conditions. Their study proposed a reference channel model for LOS and NLOS indoor conditions by deriving analytical expressions for the

probability density function (PDF) of the angle-of-arrival (AOA), the Doppler power spectral density (PSD), and the temporal autocorrelation function (ACF). Their analytical results theorized the performance of their indoor communication model and showed that the Doppler PSD of the diffuse component is symmetrical if the abscissa of the MS location equals zero, while it becomes asymmetrical if the ordinate of the MS location is equal to zero.

In 2008, Sarkar and Lo [3] conducted a propagation measurement campaign to study the performance of 802.11g in obstructed office block. The measured data from a comprehensive propagation study showed that the link throughputs of 802.11g are not always increasing with RSS in an obstructed office building.

Table I lists the key researchers and their main contributions on indoor radio propagation models and measurements.

TABLE I: KEY RESEARCHERS AND THEIR MAIN CONTRIBUTIONS IN THE STUDY OF INDOOR RADIO PROPAGATION

Researcher	Year	Main contribution
Muqaibel et al. [5]	2003	Developed propagation model for ultra-wideband (UWB) signals
Zvanovec et al. [6]	2004	Conducted indoor measurements for 2.45 GHz to predict signal propagation
Chong et al. [7]	2005	Developed and measured UWB indoor propagation channels for high-rise apartments
Sarkar and Lo [3]	2008	Conducted propagation measurements to measure IEEE 802.11g performance
Dongdong et al. [8]	2009	Studied the properties of indoor propagation for mobile communication over different wireless conditions
Ma and Patzold [9]	2010	Developed simulation models for narrowband indoor channels under LOS and NLOS conditions.
Sarkar and Lo [1]	2011	Measured 802.11g performance for various AP configuration and placement.

Papers reviewed in this section are based on indoor propagation measurements and models for wireless networks.

III. PROPAGATION ENVIRONMENT AND MEASUREMENTS

The propagation measurements results obtained from Sarkar and Lo [3] involved Wi-Fi performance measurements using wireless cards and access points in an obstructed office block at the AUT University within the School of Computer and Mathematical Sciences office building.

The transmitter (Tx) and receiver (Rx) were positioned with the Rx in different placements between A to P, and then measured under semi-LOS and NLOS conditions. RSS was calculated for each of these different positions and placements of the receiver on the floor map as depicted and illustrated in Fig. 1.

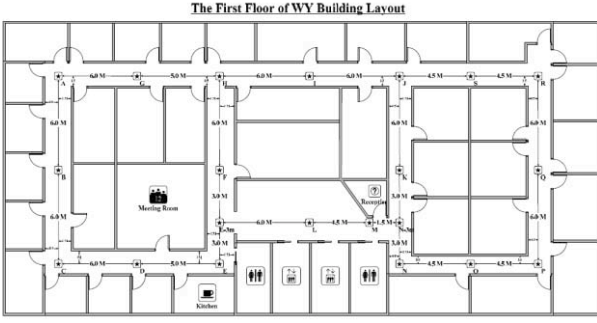


Fig. 1. Floor layout of Wi-Fi measurement Environment

The following four indoor propagation models were selected in the study to compare RSS measured values [3] with the models to find the closest match in order to answer the research question posed in Section I.

- Free-space Model
- Two-Ray Ground Reflection Model
- Shadowing – The Path Loss Model
- Shadowing – The Overall Model

IV. RESULTS AND DISCUSSION

We first consider the Free-space model to calculate the received signal strength (RSS) values using equation (1). The transmitted signal power (P_t) was set to 0.32W. The transmitter antenna gain (G_t), receiver antenna gain (G_r), and signal loss/drop not captured by the receiver (L) were set to a constant of 1. RSS denoted by signal wavelength (λ) was determined using the frequency (f) (2.462 GHz) of the wireless channel # 11.

$$P_r(d) = \frac{P_t G_t G_r \lambda^2}{(4\pi)^2 d^2 L} \quad (1)$$

RSS was calculated for each of the different positions and placements of the receiver on the floor map shown in Fig. 1 [3] for calculating signal power on receiver ($P_r(d)$) in decibel-milliwatts (dBm).

The free space model did not match with RSS measurement results for both semi-LOS and NLOS. This was as expected because the free space propagation model assumes an ideal propagation condition that there is only one clear LoS path between the transmitter (Tx) and receiver (Rx) [10].

Next, the two-ray ground model was evaluated. This model further entailed accounting to the height of the transmitting (h_t) and receiving antennas (h_r).

$$P_r(d) = \frac{P_t G_t G_r h_t^2 h_r^2}{d^4 L} \quad (2)$$

As free space model, the two-ray ground model does not match well with the propagation measurements. This was also predictable as with the two-ray ground model a single line-of-sight path between two mobile nodes is seldom the

only means of propagation. The model considers both the direct path and a ground reflection path [10].

The next model we evaluated was the shadowing path-loss model. Here β is the path-loss exponent which is usually empirically determined by field measurement.

$$\left[\frac{P_r(d)}{P_r(d_0)} \right]_{dB} = -10\beta \log \left(\frac{d}{d_0} \right) \quad (3)$$

Larger values correspond to more obstruction and hence faster decrease in average received power as distance increases [10]. Table II lists typical values for the path loss exponent (β):

TABLE II: TYPICAL VALUES OF β

Environment		β
Outdoor	Free Space	2
	Shadowed urban area	2.7 to 5
Inside of Building	Line-of-sight	1.6 to 1.8
	Obstructed	4 to 6

As the propagation measurements were carried out in an obstructed office block at the AUT University, we calculate RSS for Shadowing model by consider the path loss exponent values of 4, 5, and 6 (typical ranges for an obstructed office building). With this model, the propagation measurement results partially match for a select few placement readings of the receiver. The values did not sufficiently correspond closely to the measurements recorded in the indoor Wi-Fi for both semi-LOS and NLOS conditions. It did however fare better for certain placements of the receiver resulting in a close match unlike the previous two radio propagation models. This is because unlike the free-space and two-ray ground models, the shadowing path loss model takes into account several indoor parameters such as the channel interference, interior structure (for instance whether it is hard partition or a curved wall), signal path, etc. and thus involves several random variables.

In contrast the overall shadowing model takes this further with X_{dB} , a Gaussian random-variable with zero mean and standard deviation σ_{dB} . σ_{dB} is called the shadowing deviation and is also obtained by measurement.

$$\left[\frac{P_r(d)}{P_r(d_0)} \right]_{dB} = -10\beta \log \left(\frac{d}{d_0} \right) + X_{dB} \quad (4)$$

Table III lists typical values of shadowing deviation. Because the measurements were conducted in the obstructed office block at AUT University which made use of hard partitions, a standard deviation (σ_{dB}) of 7, alongside the Gaussian random-variable (X_{dB}) varying in value from 0 to 9.5, were considered for the analyses.

TABLE III: TYPICAL VALUES FOR STANDARD DEVIATION (σ_{dB})

Environment	σ_{dB} (dB)
Outdoor	4 to 12
Office, hard partition	7
Office, soft partition	9.6
Factory, line-of-sight	3 to 6
Factory, obstructed	6.8

The summary of research findings are presented in Table IV to VI. Table IV compares the measured RSS values with the four selected models (i.e. calculated RSS values) in semi-LOS condition. The comparative results for NLOS condition is shown in Table V.

TABLE IV: RSS MEASUREMENT VS MODELS IN SEMI-LOS CONDITION

RX Position	RSS Measurement (dBm)	RSS (dBm)			
		Propagation model			
		Overall Shadowing	Shadowing: Path Loss	Two-Ray Ground	Free-Space
B	-52.00	-51.25	-47.71	-9.03	-40.90
G	-53.00	-53.25	-57.25	-9.03	-40.90
H	-59.00	-59.22	-59.22	-19.56	-46.17
C	-60.00	-60.25	-62.25	-21.07	-46.92
I	-61.00	-60.35	-74.35	-27.12	-49.95
J	-62.00	-66.85	-84.85	-32.37	-52.56
S	-63.00	-72.06	-91.06	-35.47	-54.12
R	-65.00	-77.32	-96.32	-38.11	-55.44

TABLE V: BEST-FIT MODEL: OVERALL SHADOWING VS. PATH LOSS

RX Position	RSS Measurement (dBm)	RSS (dBm)			
		Propagation model			
		Overall Shadowing	Shadowing: Path Loss	Two-Ray Ground	Free-Space
F-H	-61.00	-60.43	-59.54	-19.71	-46.25
F-H	-62.00	-61.13	-60.10	-19.99	-46.39
F-H	-68.00	-68.12	-60.89	-20.39	-46.58
C-D	-67.00	-66.43	-62.74	-21.31	-47.05
C-D	-66.00	-65.13	-63.31	-21.59	-47.19
F	-72.00	-71.69	-79.69	-21.82	-47.30
C-D	-67.00	-66.11	-64.08	-21.98	-47.37
D	-71.00	-70.67	-66.14	-23.01	-47.89
E	-70.00	-70.85	-72.85	-26.37	-49.56
L	-77.00	-76.65	-78.65	-29.27	-51.01
J-K	-72.00	-72.93	-84.93	-32.41	-52.59
J-K	-68.00	-67.06	-85.07	-32.47	-52.62
J-K	-76.00	-75.25	-85.25	-32.56	-52.67
M	-76.00	-75.32	-85.32	-32.60	-52.69
K	-79.00	-80.00	-86.00	-32.94	-52.86
K-N	-79.00	-79.08	-87.08	-33.48	-53.12
K-N	-79.00	-79.59	-87.59	-33.73	-53.26
K-N	-82.00	-82.14	-88.14	-34.01	-53.39
N	-81.00	-81.04	-89.04	-34.46	-53.62
N-O	-87.00	-87.35	-91.35	-35.62	-54.20
N-O	-87.00	-86.48	-92.48	-36.18	-54.48
O	-90.00	-90.09	-94.09	-36.98	-54.87
O-P	-90.00	-89.14	-95.14	-37.51	-55.14
O-P	-88.00	-88.17	-96.17	-38.02	-55.40
Q-R	-70.00	-77.37	-96.37	-38.13	-55.45
Q-R	-82.00	-82.44	-96.44	-38.16	-55.47
Q-R	-75.00	-77.54	-96.54	-38.21	-55.48
Q-R	-82.00	-82.66	-96.66	-38.27	-55.53
Q	-87.00	-86.93	-96.93	-38.41	-55.59
O-P	-86.00	-85.17	-97.17	-38.52	-55.65
P-Q	-88.00	-87.51	-97.51	-38.70	-55.75
P-Q	-87.00	-87.80	-97.80	-38.84	-55.81
P-Q	-84.00	-84.11	-98.11	-38.99	-55.89
P	-84.00	-84.62	-98.62	-39.25	-56.01

Of the four indoor propagation models studied, the Overall Shadowing model resulted in the closest match with the RSS measurement results [3] followed by Shadowing

path loss model. The general trend for measured data reflects actual correlation to the radio propagation model.

Table VI summarizes the research findings by comparing the Overall Shadowing model and the Shadowing path loss model in finding out the best-fit model. We found that the mean RSS value for the Overall shadowing model matches with the measured RSS by about 94% and 99% for semi-LOS and NLOS, respectively.

We also observe that the Overall shadowing model is better (in terms of best-fit) than the Shadowing path loss model by about 16.8% and 10.3%, for semi-LOS and NLOS, respectively.

Another observation is that both the Overall Shadowing and the Shadowing path loss models perform well (in terms of achieving closest match with the measured RSS) in NLOS than Semi-LOS condition. This is because of the characteristics of Shadowing models as they predict the behavior of obstructed office environment very well.

The main conclusion is that the Overall shadowing model is the best-fit for both semi-LOS and NLOS conditions.

TABLE VI: BEST-FIT MODEL: OVERALL SHADOWING VS. PATH LOSS

Model	% of matching with RSS measurement values		Shadowing fits well in NLOS condition (%)
	Semi-LOS	NLOS	
Overall Shadowing	94.4	98.9	4.6
Shadowing Path loss	78.5	88.7	11.5
Overall Shadowing best-fits (%)	16.8	10.3	

V. ANALYSIS OF RESEARCH FINDINGS

In Fig. 2, we plot RSS against distance for semi-LOS. One can observe that the overall shadowing model matches closest to the measured RSS, followed by the path loss and free space models. The two-ray ground model is the least effective. This is because the model itself is best known for accurate prediction of signal propagation at a longer distance than the free space model, occurring mainly due to the oscillation caused by constructive and destructive combination of the two rays. The testbed network was in an obstructed office block located at the AUT University building. Unlike the free-space model which assumes ideal propagation conditions with clear line-of-sight between transmitter and receiver, the testbed wireless network involved a complex indoor environment including use of hard-partitions and as such a lower signal strength at the receiver. This thus involved use of a model that would factor in the external variables responsible for signal attenuation and such. The overall shadowing model was thus the most appropriate match for the indoor propagation RSS measurement results.

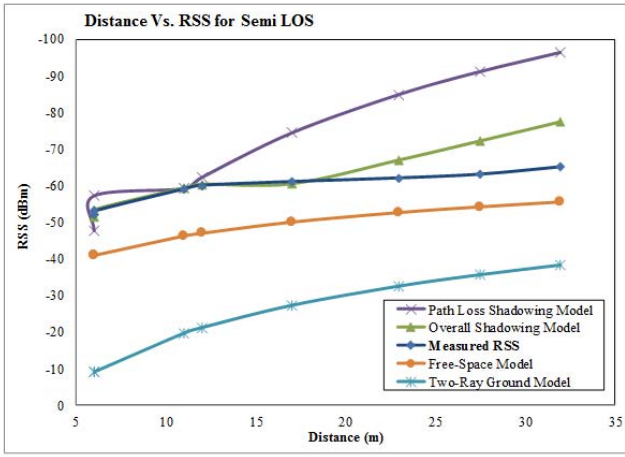


Fig. 2. Distance versus RSS for semi-LOS: Comparison of measured and four selected models (free space, two-ray ground, path loss shadowing, and overall shadowing).

In Semi-LOS conditions, the overall shadowing model was accurate to the measured RSS for Tx-Rx distances set at less than 10m when the path loss exponent was 6 and XdB ranged between 2 and 3. When Tx-Rx separation is between 10 to 15m, the overall shadowing model was most accurate to the measured RSS when the path loss exponent was 4 and XdB between 0 and 1. For Tx-Rx separation between 15 to 25m, the overall shadowing model was accurate to the measured RSS for the path loss exponent of 4 and XdB between 7 and 9. For Tx-Rx separation greater than 25m, the overall shadowing model was most accurate for the path loss exponent of 4 and XdB of 9.5.

Fig. 3 compares measured RSS with the four selected indoor models for NLOS condition. The overall shadowing model was accurate to the measured RSS for Tx-Rx separation of 15m for path loss exponent of 5 and XdB ranged between 4 and 7. When the Tx-Rx separation ranged from 15 to 25m, the overall shadowing model was most accurate to the measured RSS for the path loss exponent of 4 and XdB of 1. For TX-RX between 25 to 30m, the overall shadowing model was accurate to the measured RSS for the path loss exponent of 4 and XdB was set to 2. For Tx-Rx distance greater than 30m, the overall shadowing model was most accurate when the path loss exponent was 4 and XdB was between 3 and 9.5.

The overall shadowing model estimates propagation to be slightly higher in Semi-LOS conditions if the path loss exponent is 4 and XdB the Gaussian random variable is 9.5 for Tx-Rx distances less than 10m. This would then result with higher RSS of -19.16 dBm, a significant improvement to the recorded RSS of -51.25 dBm. It also estimates propagation to be slightly higher if the path loss exponent is 4 and XdB the Gaussian random variable is 9.5 for instances where the Tx-Rx distance is between 10 to 15m if the path loss exponent is 4 and XdB is 9.5. This would then result with higher RSS of -40.22 dBm, a significant improvement to the recorded RSS of -59.22 dBm.

For Tx-Rx separation greater than 15m, the recorded RSS in Semi-LOS conditions is the most efficient and matches the best possible RSS predicted by the overall shadowing

model. In the case of NLOS condition, the overall shadowing model estimates propagation to be slightly higher if the path loss exponent is 4 and XdB is 9.5 for Tx-Rx separation of 10 to 15m. This would then result with a higher RSS of -40.54 dBm, a significant improvement to the recorded RSS of -60.42 dBm.

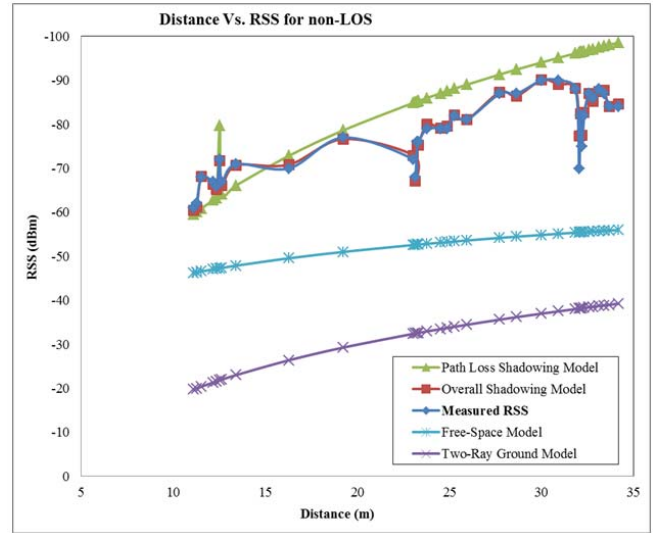


Fig. 3. Distance versus RSS for NLOS: Comparison of measured and four selected models (free space, two-ray ground, path loss shadowing, and overall shadowing).

Propagation is also predicted to be slightly higher when the path loss exponent is 4 and XdB is 9.5 when Tx-Rx distance is between 15 to 25m if the path loss exponent is 4 and XdB is 9.5. This would then result with higher RSS of -53.84 dBm, a significant improvement to the recorded RSS of -70.67 dBm.

For measurements with Tx-Rx separation between 25 and 30m, propagation could be slightly higher when the path loss exponent is 4 and XdB is 9.5. This would then result with higher RSS of -53.84 dBm, a significant improvement to the recorded RSS of -70.67 dBm.

For Tx-Rx separation greater than 30m, propagation can be slightly improved for path loss exponent of 4 and XdB of 9.5. This results in higher RSS of -75.08 dBm, a significant improvement to the recorded RSS of -90.08 dBm. This decreased in RSS for increased Tx-Rx separation can be attributed to the waveguide effect [3].

VI. CONCLUSIONS

This paper addressed the following research question. What indoor radio propagation model “best-fits” with the measurement results? We compared RSS measurement results (obtained in the obstructed office block at AUT University) with the calculated RSS values for Free-space, Two-ray ground reflection, shadowing path loss, and the overall Shadowing models, to find the possible best-fit. Results obtained have shown that the overall shadowing is the best-fit model (closest match) with the measured data followed by Shadowing path loss model for both semi-LOS and NLOS conditions. To quantify the best-fit (closest

match) with the measurements, we compared the mean RSS values of Overall Shadowing model and the Shadowing path loss model. Our findings showed that the mean RSS values obtained from the Overall shadowing model matches with the measured RSS by about 94% and 99% for semi-LOS and NLOS, respectively. We found that the Overall shadowing model is better (in terms of best-fit) than the Shadowing path loss model by about 16.8% and 10.3%, for semi-LOS and NLOS, respectively. Quantifying the best-fit RSS measurement with outdoor propagation models is suggested as an extension to the work presented here.

REFERENCES

- [1] N. I. Sarkar and E. Lo, "Performance studies of 802.11g for various AP configuration and placement," presented at the 2011 IEEE Symposium on Computers and Informatics (ISCI 2011), Kuala Lumpur, Malaysia, March 20 - 22, 2011, pp. 29-34.
- [2] N. I. Sarkar, "The impact of transmission overheads on IEEE 802.11 throughput: analysis and simulation," *Journal of Selected Areas in Telecommunications (JSAT)*, vol. 2, no. 3, pp. 49-55, 2011.
- [3] N. I. Sarkar and E. Lo, "Indoor propagation measurements for performance evaluation of IEEE 802.11g," presented at the IEEE Australasian Telecommunications Networks and Applications Conference (ATNAC '08), Adelaide, Australia, December 7-10, 2008, pp. 163-168.
- [4] N. I. Sarkar and K. W. Sowerby, "Wi-Fi performance measurements in the crowded office environment: a case study," presented at the 10th IEEE International Conference on Communication Technology (ICCT '06), Guilin, China, November 27-30, 2006, pp. 37-40.
- [5] A. H. Muqaibel, A. Safaai-Jazi, A. M. Attiya, A. Bayram, and S. M. Riad, "Measurement and characterization of indoor ultra-wideband propagation," presented at Ultra Wideband Systems and Technologies, 2003 IEEE Conference on, 16-19 Nov. 2003, 2003, pp. 295-299.
- [6] Zva, x, S. novec, M. Valek, and P. Pechac, "Results of indoor propagation measurement campaign for WLAN systems operating in 2.4 GHz ISM band," presented at Antennas and Propagation, 2003. (ICAP 2003). Twelfth International Conference on (Conf. Publ. No. 491), 31 March-3 April 2003, 2003, pp. 63-66 vol.1.
- [7] C.-C. Chong, Y.-E. Kim, S. K. Yong, and S.-S. Lee, "Statistical characterization of the UWB propagation channel in indoor residential environment," *Wireless Communications and Mobile Computing*, vol. 5, no. 5, pp. 503-512, 2005.
- [8] D. Zeng, g. Lu, and J. Lin, "Measurement at 820MHz for indoor wave propagation," presented at Environmental Electromagnetics, 2009. CEEM 2009. 5th Asia-Pacific Conference on, 16-20 Sept. 2009, 2009, pp. 204-207.
- [9] M. Yuanyuan and M. Patzold, "Design and Simulation of Narrowband Indoor Radio Propagation Channels under LOS and NLOS Propagation Conditions," presented at Vehicular Technology Conference (VTC 2010-Spring), 2010 IEEE 71st, 16-19 May 2010, 2010, pp. 1-7.
- [10] T. Henderson. (2011). *18.1 Free space model*, from <http://www.isi.edu/nsnam/ns/doc/node217.html>